

## Damage Information Mapping from Images to BIM Models for the Detection of Ancient Stone Bridges

Yingkui Sun<sup>1,2</sup>, Miaole Hou<sup>1,2</sup>, Huiwen Chen<sup>1,2</sup>, Censhan Gao<sup>1</sup>, Aliea Nallbani<sup>1,2</sup>

<sup>1</sup> School of Geomatics and Urban Spatial Informatics, Beijing University of Civil Engineering and Architecture, Beijing 102616, China - 2108160123002@stu.bucea.edu.cn, houlmiaole@bucea.edu.cn

<sup>2</sup> Beijing Key Laboratory for Architectural Heritage Fine Reconstruction Health Monitoring, No.15 Yongyuan Road, Daxing District, Beijing, China - 2108160123002@stu.bucea.edu.cn, houlmiaole@bucea.edu.cn

**Keywords:** Ancient Stone Bridge, Building Information Modeling (BIM), Damage, Mapping, Digital Preservation.

### Abstract

Ancient stone bridges, as precious cultural heritage, carrying the deep historical memory and craft traditions of the Chinese nation, are susceptible to spalling, cracks and other damages due to the long-term impact of traffic load, environmental erosion, natural aging, and human damage. The traditional manual detection method is inefficient, subjective and lacks a standardized assessment system. Therefore, this paper proposes an intelligent detection and digital management method of ancient stone bridge damage by integrating image recognition and Building Information Modeling (BIM), and constructs an integrated technical process of "recognition-conversion-mapping". The method uses deep learning model to realize pixel-level segmentation and feature extraction of bridge damage, develops multi-scale spatial coordinate conversion method to map the real damage location into BIM model, and establishes relevant damage components to realize visual management.

### 1. Introduction

With the successful bidding of the Beijing Central Axis, the importance of the Wanning Bridge, as the oldest bridge on the central axis, has become more prominent. However, this ancient bridge has begun to develop various problems as it has been used for more years. Some problems affect the appearance, while others threaten the structural safety of the bridge. Failure to detect these problems in a timely manner may result in the continued deterioration of the bridge's condition or even serious consequences. Therefore, it is very necessary to inspect and manage bridge problems regularly so that effective measures can be taken in time. This is not only related to the conservation of old bridges, but also to the safety of tourists. At present, the inspection of problems of ancient bridges mainly relies on manual visual inspection and manual records. Inspectors judge the type of problems by experience and register the problems with a form. This method relies too much on personal experience and is prone to errors, leading to inaccurate inspection results and inefficient maintenance. Moreover, manual inspection requires a lot of labor and time, which is very costly. To realize accurate and efficient management of ancient bridge problems, automated inspection methods must be developed.

Wanning Bridge is both a major transportation route and a popular attraction, receiving a large number of tourists every day. These multiple attributes of the traditional manual inspection have brought great challenges. However, compared with other large-scale ancient buildings, Wanning Bridge has an obvious advantage: the bridge is small, and daily inspection can cover every corner of the bridge. This feature provides a possibility for image-based digital inspection. Using image records instead of manual inspection can not only avoid subjective judgment errors but also reduce the professional threshold; ordinary staff can complete the filming work after simple training. However, the focus of the current research remains in the automatic inspection stage, and there is still a lack of effective programs for

the systematic management and in-depth application of inspection data.

BIM technology is a core tool for building information management(Zou et al., 2017). It can integrate building data and information data together and realize data sharing in the whole life cycle of the building(Pocobelli et al., 2018). BIM can fully demonstrate the functional characteristics of the building. A large amount of data is generated during the use of a building(Sharafat et al., 2021), and integrating this data into a BIM model can optimize data management and support building maintenance. It has been proven that integrating monitoring data, structural features, and other information into BIM models can significantly improve management efficiency(Khan et al., 2022). Mapping various data into BIM models can provide a clearer understanding of the status of each component and provide a scientific basis for monitoring and maintenance. However, most of the problem information detected at present is only used to generate paper reports and is not deposited into the digital model for real-time monitoring and management. Although BIM technology has been applied in building management, there is still a lack of mechanisms to correlate the actual building status with the BIM model in real time. Combining the object management of BIM with the actual building can not only promote the application of NDT technology but also reflect the inspection results into the BIM model for management. This information mapping management can provide accurate and efficient technical support for building monitoring and maintenance.

Based on the above ideas, this paper proposes a new method: combining bridge images and BIM models to identify, locate and manage the problems of Wanning Bridge. The specific steps are: firstly, automatically detect the bridge damage using image recognition technology to determine the size and location of the damage; then develop a coordinate conversion method to correspond the damage location in the image to the BIM model; finally, store all the detected damage information into the BIM

model. Finally, all the detected problem information is stored in the BIM model. By integrating the actual inspection data with the BIM model, it provides support for bridge monitoring and maintenance.

After the introduction, this paper is organized as follows: section 2 reviews the related research; section 3 details the proposed detection method and BIM mapping steps; section 4 verifies the feasibility of the method through actual cases; and finally, it summarizes the research results, pointing out the shortcomings and future research directions.

## 2. Related Work

### 2.1 Image-Based Facility Inspections

Imagery (e.g., social media pictures, public camera data, street view images, etc.) offers new possibilities for automated inspection of facilities. By integrating image data, researchers are able to realize large-scale infrastructure monitoring and defect identification in a cost-effective and high-coverage manner.

Using a combination of image processing and terrestrial laser scanning (TLS) based techniques, (Huang et al., 2018) proposed a new method, MCrack-TLS, for automated assessment of cracks in concrete bridges and (Hawari et al., 2018) presented the development of an automated tool using image processing techniques and several mathematical formulas for analyzing the output data from closed-circuit television (CCTV) camera images for the detection of several defects in sewer pipes. (Jeong et al., 2020) evaluates the application of unmanned aerial vehicle (UAV) photogrammetry in reconstructing 3D models of traditional wood-frame building dimensional measurements. (Cheng et al., 2024) developed a HyBridGAN model to detect building components (i.e., columns and structural walls), categorize building damage types, and determine the extent of building damage. (Garrido et al., 2019) introduced the first method to automatically detect areas of moisture affecting the surfaces of building materials, preventing moisture from damaging the building. (Wang et al., 2018) proposes a new method for automatic inspection of tool parts for industrial equipment, which realizes automatic inspection of disposable blades in precision cutting. In addition, images have been used for trait detection in plants (Pound et al., 2017); defect inspection of products in the plastics industry (Liang et al., 2019) and inspection work of underwater scenes (O'Byrne et al., 2020), etc.

These existing studies have shown that the use of images is possible to produce good results in various kinds of damage detection. However, there is still limited research on how to manage and utilize this detected damage information.

After obtaining the damage detection results, the results are mapped to the BIM model. This process is necessary to view and manage the detection results and to take appropriate action on them. In the mapping process, coordinate transformation is an important step to convert the location of the detected data in the real world (e.g., bridge damage) to the corresponding location in the BIM model.

### 2.2 BIM-Based Management

The combination of BIM and management significantly improves project efficiency and quality by integrating building information with project management processes. It also aids risk

management, facility maintenance and sustainability analysis, optimizes design and extends the building lifecycle. (Lu et al., 2020)(Kaewunruen et al., 2018)(Zhao et al., 2022)(Kaewunruen et al., 2018)investigated the feasibility of combining BIM with digital twins in project management, which can improve the efficiency as well as the automation of monitoring. (Delgado et al., 2020)provides practitioners with the necessary information to guide adoption decisions by investigating the use of BIM for vr and ar. (Lyu et al., 2019) provides the necessary information to guide the adoption decisions by using a BIM model in conjunction with the GIS, RS combined with scenario analysis to propose a prospective approach for assessing flood risk in metro systems. (Franz et al., 2017) explored a research analysis on the status of the impact of BIM combined with other aspects of project delivery on team integration. (Zhou et al., 2020) combined BIM with a variety of relevant data metrics to analyze to assess and manage risks during the construction of undersea tunnels. (Zhang et al., 2022) combined BIM with lod to improve the quality and efficiency of construction including BIM-based digital representation, the Internet of Things (IoT), data storage, integration, and analytics, as well as interaction with the physical environment, and to improve construction safety. (Shahi et al., 2019)investigated the use of BIM for several smart city management applications including city-level plan review, integrated logistics planning and smart city asset management.

It can be seen that the research management study on the integration of BIM with the damage information of bridge types, especially ancient stone bridges, is smack full of limitations. However, this information has an important value for the conservation and maintenance of buildings, and similarly, the research is slightly insufficient in terms of BIM management.

## 3. Research on Bridge Damage Detection and BIM Model Mapping Methods

Figure 1 shows the process framework for damage detection and mapping of ancient stone bridges based on image acquisition and BIM integration, which has four parts. The first part is the acquisition and preparation of image data, the second part is the detection of the damage as well as the localization, the third part is the conversion between the relevant coordinates, and the fourth part is the mapping of the damage to the established BIM model.

### 3.1 Pre-Preparation and Data Acquisition

**3.1.1 Preliminary:** Preparation work is divided into three parts, The first part is the pre-shooting preparation. Including 1, the use of camera models, 2, shooting location time selection (because it is a scenic spot and traffic, so there may be tourists and vehicles interference), 3, field visits to assess the site conditions to evaluate the potential factors that may exist.

The second part is to determine the segmentation area and the center point based on the BIM model of the bridge. Specifically, Dynamo is used to extract the corner coordinates of each part.

The third part is to develop the shooting plan for the bridge. Including 1, camera shooting route planning 2, according to the BIM model segmentation to determine the size of the camera FOV, and then deduce the vertical distance between the camera and the object (because the bridge body belongs to the irregular

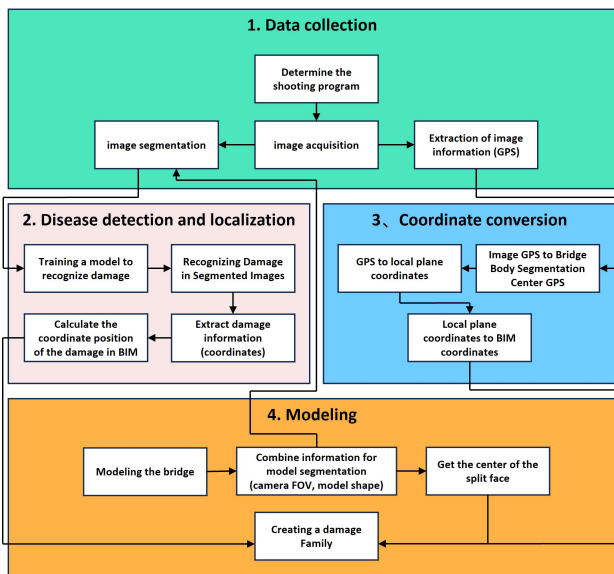


Figure 1. Bridge damage detection and mapping process.

model, so you need to determine the camera's shooting orientation as far as possible in the appropriate segmentation model to reduce the workload of the later coordinate conversion)

This part of the need for the camera to meet certain requirements, the need for a stabilizer, positioning function, high resolution, and the need for the camera to meet certain needs. This part of the camera needs to meet certain requirements, needs to have a stabilizer, positioning function, high resolution, portability, and then needs to determine the size of the camera FOV according to the partition of the BIM model, which is one of the keys to the overall bridge damage detection. This is one of the keys to the overall bridge damage detection. We determine the FOV width based on the segmented model and then determine the height of the camera and the vertical distance from the bridge. So for this part we need to get the dimensions of the segmented model, the dimensions of the field, the sensor size, and the focal length of the camera.

To extract the distance between the photo and the actual bridge, we need the dimensions of the segmented part of the bridge (i.e., the dimensions of the field of view) based on the triangular similarity, combined with the dimensions of the camera's sensor.

The sensor size of the camera is set to  $S$ , the distance between the camera and the bridge is set to  $D$ , and the focal length of the camera is  $f$ . According to the formula for the actual range of the field of view FOV:

$$FOV = \frac{S \times D}{f} \quad (1)$$

The distance between the camera and the bridge can be obtained as:

$$D = \frac{FOV \times f}{S} \quad (2)$$

**3.1.2 Data Acquisition Process:** After the completion of the preliminary work, the bridge data were collected using a

mobile phone, and in the process of photographing the bridge, the plane of the mobile phone should always be parallel to the stone fence lookout columns of the bridge, to ensure that the lens is directly facing the stone fence, and to prevent image aberrations due to the camera's angle of view shift, as shown in Figure 2.

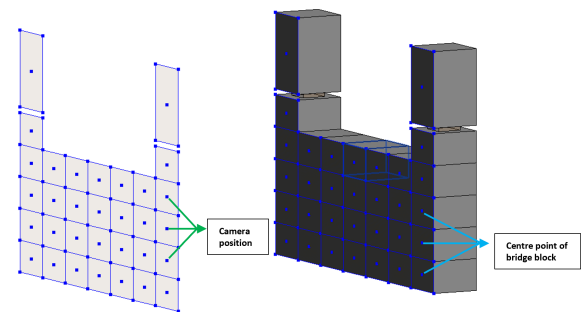


Figure 2. Shooting position with the centre of the bridge chunks.

After acquiring the image data at the points planned in the preparatory work, name all the image data in a specified order and store them in a format that can be used, checking the images for the presence of an ExIf (Exchangeable Image file) The function of an ExIf is to record the shooting information such as the shutter speed, aperture value, and so on, and it can even include global positioning information. Then we use Python to develop an algorithm to automatically extract the ExIf information contained in the image and filter out the required information (latitude, longitude, elevation, size, image orientation, etc.) and package the extracted information into a data table, as shown in Figure 3.

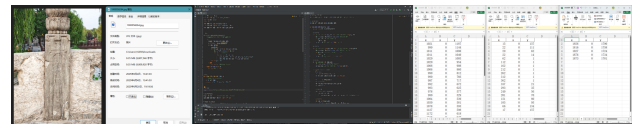


Figure 3. Coordinate information extraction process.

We collect the images one by one according to the pre-set shooting points. After shooting, all images need to be renamed sequentially and saved in a common format. At the same time, we need to check whether the images contain Exif information, which is the shooting data stored in the images, including shutter speed, aperture size, etc., and in some cases, GPS location data will also be recorded. Next, you need to write a program in Python. This program should be able to automatically read the Exif information in the image and filter out the data we need from it, including longitude, latitude, altitude, picture size, and shooting direction. Finally, the program has to organize this extracted information into a tabular form.

### 3.2 Coordinate Transformation

The coordinate transformation is divided into three parts, the first part is to convert the coordinates of the camera to the actual coordinates of the wall, the second part is to convert the latitude and longitude coordinates of the wall to the specified plane coordinates, and the third part is to convert the plane coordinates to the coordinates in the model.

### 3.2.1 Camera Coordinates Are Converted to the Coordinates of the Center of the Corresponding Bridge Section:

Objective: To calculate the latitude, longitude, and height of the center point of the corresponding bridge area based on the latitude and longitude of the camera's shooting point. Known data: 1. the latitude and longitude ( $\phi_{Li}, \phi_{Bi}$ ) of the camera's shooting point a, and the height of the camera; 2. the latitude and longitude ( $\lambda_{Li}, \lambda_{Bi}$ ) of the point B of the corresponding bridge region, which is measured by rtk; 3. the perpendicular distance  $L$  between the camera and the bridge body, which is measured by a laser or by some other means; and 4. the average radius of the earth  $R = 6,371,393\text{M}$ .

1. Firstly, perform the calculation of the spherical angle  $c$  between the camera and the corresponding bridge region.

$$c = \arccos(\sin\lambda_{Bi}\sin\phi_{Bi} + \cos\lambda_{Bi}\cos\phi_{Bi}\cos(\lambda_{Li} - \phi_{Li})) \quad (3)$$

2. Calculate the azimuth of the camera  $a$

$$\alpha = \text{atan2}(\sin(B_L - A_L) \cos B_B, \cos A_B \sin B_B - \sin A_B \cos B_B \cos(B_L - A_L)) \quad (4)$$

3. Calculate the latitude of the center point corresponding to the bridge area  $\lambda_{Bi}$

$$\delta = \frac{L}{R} \quad (5)$$

$$\lambda_{Bi} = \arcsin(\sin\phi_{Bi}\cos\delta + \cos\phi_{Bi}\sin\delta\cos\alpha) \quad (6)$$

4. Calculate the longitude of the center point corresponding to the bridge area  $\lambda_{Li}$

$$\lambda_{Li} = \phi_{Li} + \text{atan2}(\sin\alpha\sin\delta\cos\phi_{Bi}, \cos\delta - \sin\phi_{Bi}\sin\lambda_{Bi}) \quad (7)$$

5. Height correction Because the height is actually measured by the level measurement. Because the height is actually measured by the level measurement, it is easy to be converted inaccurately due to the camera shooting error, so according to the position of each shooting point on the bridge body on the BIM model, it is directly assigned to the center point of the corresponding bridge body area in the segmentation. Finally, a Python code was developed to automate the input and output of the coordinate conversion.

### 3.2.2 Conversion of WGS-84 Coordinates to Planar Coordinates:

Objective: To convert latitude and longitude (WGS-84 coordinates) into a local plane rectangular coordinate system (X-Y plane) associated with the bridge body. Known data: 1. Latitude and longitude (WGS-84) ( $\phi_{Li}, \phi_{Bi}$ ) of the segmented area of the bridge body; 2. Parameters of the Earth's ellipsoid, with the long axis  $a=6,378,137\text{M}$  and the short axis  $b=6,356,752\text{M}$ . Define the X-axis as a latitudinal (east-west) direction, and define the Y-axis as a meridional (north-south) direction. 1. Choose the latitude and longitude ( $\phi_{L0}, \phi_{B0}$ ) (WGS-84 coordinates) as the origin of the plane coordinates. The reason for using the local coordinate system is that the UTM projected coordinates have the effect of the band number and are applicable to a wide range of areas, and it is simpler and more efficient to use the local plane coordinate system for the actual bridge size. 2. Calculate the plane coordinates of  $B_0$  ( $\phi_{x0}, \phi_{y0}$ ) In the x-axis direction, considering the radius of curvature of the earth  $R_x = \frac{a}{\sqrt{1-e^2\sin^2(\lambda_{B0})}}$ ,  $e^2 = \frac{a^2-b^2}{a^2}$  the calculation will be complicated, and the bridge body is relative to the overall earth, the earth's curvature length of 100 meters

of the earth. The height difference of the earth's sphere brought about by the 100 meters of the earth's arc length is only 0.8 mm, which is much lower than the actual required accuracy, so the distance between two points on the bridge can ignore the influence brought about by the radius of the earth's curvature, and so the plane coordinates in the direction of the x-axis can be simplified in an approximate way to be

$$\lambda_{x0} \propto \frac{a^2}{\sqrt{a^2 + b^2 \cdot \tan^2(\lambda_{B0})}} \quad (8)$$

Similarly, the plane coordinates in the direction of the y-axis can be approximately transformed into

$$\lambda_{y0} \propto \frac{b^2}{\sqrt{b^2 + a^2 \cdot \cot^2(\lambda_{B0})}} \quad (9)$$

3. Calculation of plane coordinates of points in other divided areas on the bridge If the coordinates of points in other areas on the bridge are in the same longitude, the longitude is unchanged, y is unchanged in plane coordinates, and only the latitude changes.

$$\lambda_{xi} = \lambda_{x0} \quad (10)$$

$$\lambda_{yi} = \lambda_{y0} + \Delta\lambda_B \cdot R \cdot \frac{\pi}{180^\circ} \quad (11)$$

Similarly, for those at the same latitude, only the change in longitude

$$\lambda_{xi} = \lambda + \Delta\lambda_L \cdot R \cdot \cos(\lambda_{B0}) \cdot \frac{\pi}{180^\circ} \quad (12)$$

$$\lambda_{yi} = \lambda_{y0} \quad (13)$$

For simultaneous changes in latitude and longitude, superimpose the two changes above.

$$\lambda_{xi} = \lambda_{x0} + \Delta\lambda_L \cdot R \cdot \cos(\lambda_{B0}) \cdot \frac{\pi}{180^\circ} \quad (14)$$

$$\lambda_{yi} = \lambda_{y0} + \Delta\lambda_B \cdot R \cdot \frac{\pi}{180^\circ} \quad (15)$$

Within a small variation of the bridge, the longitudinal component of latitude and the latitudinal component of longitude can be ignored, and only the component in the principal direction can be superimposed.

### 3.2.3 Mapping of Planar Coordinates to BIM Model Coordinate System:

Objective: Transform the coordinates in the local plane coordinate system to the local coordinate system in the BIM model through affine transformation, and realize the accurate mapping of the location of the bridge body's damage to the BIM model. Known data: 1) the coordinates of the midpoints in the segmented area under the local plane coordinate system ( $\lambda_{xi}, \lambda_{yi}$ ); 2) the coordinates of the midpoints in the segmented area of the corresponding BIM model ( $\lambda'_{xi}, \lambda'_{yi}$ ) Because the BIM model uses the coordinate system in the model world, and there is an error between the model size and the real size when the model is built, and there is also a difference between the orientation of the model in the model world and the real world. Therefore, we need to use a transformation method to convert the coordinates in the local plane coordinate system to the corresponding coordinates in the BIM model. When transforming two planar coordinate systems to each other, there are translations, rotations, scaling, and shearing from the bridge planar coordinate system to the model world coordinate system. After the transformation, it is necessary to make sure that the points before the transformation are on a straight line,



and after the transformation, they should also be on a straight line. The two lines of the original coordinate system before the transformation should be parallel, and the two lines of the transformed coordinate system should also be parallel. The ratio of the two segments of a line above the original coordinate system before the transformation remains unchanged after the transformation. So we need to use affine transformation formulas to solve the problem of translation, rotation, scaling, and shearing. The original coordinates  $(x, y)$  become a matrix form  $\begin{bmatrix} x \\ y \end{bmatrix}$ , where the three transformations, rotation, scaling, and shear, are called linear transformations, and are represented by the four parameters  $a, b, c, d$ . Any linear transformation can be realized using a  $2 \times 2$  matrix represented by these four parameters  $A = \begin{bmatrix} a & b \\ c & d \end{bmatrix}$ . But in translational transformations,  $\mathbf{v}' = \mathbf{v} + \mathbf{t}$  cannot be represented by a matrix. So the four transformations of rotation, scaling, shearing, and translation have to be upscaled, so the final complete transformation matrix is:

$$M = \begin{bmatrix} A & \mathbf{t} \\ 0^T & 1 \end{bmatrix} = \begin{bmatrix} a & b & t_x \\ c & d & t_y \\ 0 & 0 & 1 \end{bmatrix} \quad (16)$$

$A$ : the linear transformation part of the coordinates;  $t$ : the translation part of the coordinates.

$$\begin{bmatrix} x' \\ y' \\ 1 \end{bmatrix} = \begin{bmatrix} a & b & t_x \\ c & d & t_y \\ 0 & 0 & 1 \end{bmatrix} \begin{bmatrix} x \\ y \\ 1 \end{bmatrix} = \begin{bmatrix} ax + by + t_x \\ cx + dy + t_y \\ 1 \end{bmatrix} \quad (17)$$

Simplify it to:

$$\begin{cases} x' = ax + by + t_x \\ y' = cx + dy + t_y \end{cases} \quad (18)$$

There are six transformation parameters, including four linear transformation parameters:  $a, b, c, d$ ; two translation transformation parameters:  $t_x, t_y$ . Therefore, we need three sets of coordinates before and after the transformation to solve for the unknown parameters, before the transformation:  $(x_1, y_1), (x_2, y_2), (x_3, y_3)$ ; after the transformation:  $(x'_1, y'_1), (x'_2, y'_2), (x'_3, y'_3)$ , obtained by substituting the points into the simplified formula:

$$\begin{cases} x'_1 = ax_1 + by_1 + t_x \\ x'_2 = ax_2 + by_2 + t_x \\ x'_3 = ax_3 + by_3 + t_x \\ y'_1 = cx_1 + dy_1 + t_y \\ y'_2 = cx_2 + dy_2 + t_y \\ y'_3 = cx_3 + dy_3 + t_y \end{cases} \quad (19)$$

### 3.3 Damage Detection

In this study, the mask R-CNN framework is applied to the field of surface damage detection of stone cultural relics. In the experimental testing phase, the model successfully realizes the accurate identification and pixel-level annotation of common flake flaking damage on the surface of ancient bridges based on its powerful instance segmentation capability. The experimental results are shown in Figure 4. Through the end-to-end deep learning architecture, the model can effectively extract the multi-scale features of the damage region and maintain high detection accuracy under the complex background interference, which fully verifies the technical advantages and application

potential of deep learning-based target detection and instance segmentation technology in the intelligent recognition of cultural relics damage.



Figure 4. Examples of damage recognized by Mask R-CNN.

### 3.4 Damage Localization

Masks for instance segmentation are obtained from the damage result images recognized using Mask R-CNN, and then the masks of the target damage instances are extracted, and coordinate recognition is performed after the masks are converted into a format that allows coordinate recognition. The contour coordinate information of the damaged area is extracted from the mask data output from the Mask R-CNN. These coordinate data are based on the computer vision coordinate system, i.e., a two-dimensional coordinate system with the upper-left corner of the image as the origin  $(0,0)$ , horizontally to the right as the positive direction of the  $x$ -axis, and vertically down as the positive direction of the  $y$ -axis. So we need to carry out the conversion of the computer vision coordinate system into a coordinate system with the center of the image as the origin. The process of coordinate conversion: In the annotation of the damage results of the image, the coordinate system used on the image is the computer vision coordinate system, which is based on the upper-left corner of the image as the origin, to the right of the  $x$ -axis in the positive direction, and down for the  $y$ -axis in the positive direction, which is different from the local planar coordinate system used in the present study, which is based on the geometrical center of the image as the origin, so that the coordinates of the identified contours are mapped onto the model in the present study. In this study, the mapping of the identified contour coordinates to the model requires a coordinate transformation with the center of the image as the origin. 1. Calculation of the center point of the computer vision coordinate system The resolution of the original image is  $310 \times 310$  px, then the center point of the image is:

$$x_{\text{center}} = \frac{310}{2} = 155\text{px}, y_{\text{center}} = \frac{310}{2} = 155\text{px} \quad (20)$$

2. Extracting the coordinates (pixel points in the figure) in one of the masks of the damage detected by the Mask R-CNN (the coordinate system for this coordinate has the upper left corner of the image as the origin of the computer vision coordinate system), as shown in Table 1.

Number	X	Y
1	162.3152709359605	244.2118226600985
2	164.9014778325122	245.4433497536945
3	166.9950738916256	242.9802955665024
...	...	...

Table 1. Original coordinates extracted from the image.

3. Convert the image center point to the origin of the coordinate system as shown in Table 2, Figure 5. Set the center point of the image to the coordinate origin  $(0,0)$ , with  $x$ -positive to the right

and y-positive to the top. For each coordinate point in the mask ( $x_{\text{defect}}, y_{\text{defect}}$ ), the coordinates in the new coordinate system are

$$x_{\text{new}} = x_{\text{defect}} - x_{\text{center}} \quad (21)$$

$$y_{\text{new}} = -(y_{\text{defect}} - y_{\text{center}}) \quad (22)$$

So the coordinates in the mask are in the new coordinate system after the transformation:

$$x_{\text{new}} = 162.31527093596057 - 155 = 7.31527093596057\text{px} \quad (23)$$

$$y_{\text{new}} = -(244.2118226600985 - 155) = -89.2118226600985\text{px} \quad (24)$$

Number	X	Y
1	7.3152709359605	-89.2118226600985
2	9.9014778325122	-90.4433497536945
3	11.9950738916256	-87.9802955665024
...	...	...

Table 2. Transformed coordinates.

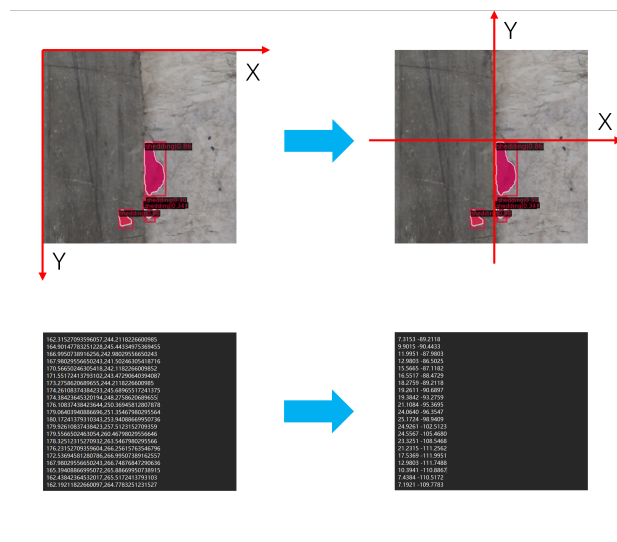


Figure 5. Image coordinate conversion.

### 3.5 Mapping Bridge Damage to BIM Models

After identification and coordinate transformation, the coordinate data of each mask coordinate of the damage on the model were obtained, which were stored in the database, and using Dynamo and Python scripts, the coordinates of the damage were read from the database and the corresponding 3D damage model blocks were automatically generated. Finally, these damage model blocks are accurately added to the bridge body model according to coordinate matching. The whole process realizes the automatic 3D visualization of damage modeling. The damage model blocks are accurately embedded into the bridge model according to the actual coordinates and scale, so that the spatial distribution and dimensional characteristics of the damage are visualized, which is convenient for the subsequent visual analysis and operation and maintenance management, as shown in Figure 6.

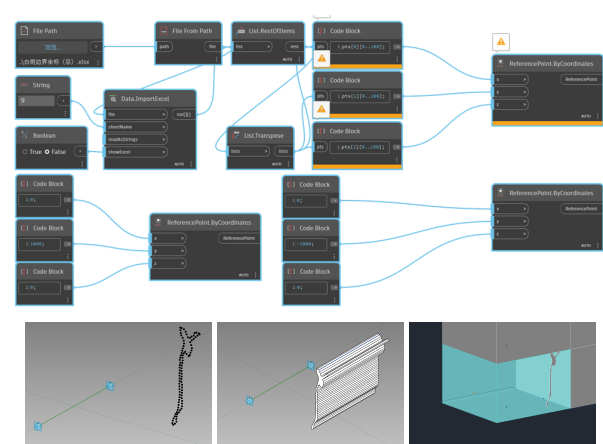


Figure 6. Damage family creation mapping process.

## 4. Case Studies

This study proposes a method to combine damage data of ancient stone bridges with BIM models. In order to verify the effectiveness of the method, the west side of the Wanning Bridge of the Beijing Central Axis facing the roadway railing, as shown in Figure 7, was selected for testing in this study.



Figure 7. Real bridge.

### 4.1 Image Data Extraction

First, the photographed object was placed in the center of the camera's viewfinder frame to minimize the effect of perspective distortion, and each baluster was photographed individually. Then, the GPS information of the images was extracted using Python, followed by segmenting and numbering the images according to the model. Finally, this processed image information was stored in a database. Some of the data is shown in Table 3.

Number	Longitude	Latitude
1	116.38997440	39.93508062
2	116.38997471	39.93507793
3	116.38997502	39.93507524
...	...	...

Table 3. GPS information extracted from images.

### 4.2 Coordinate Conversion

The coordinate data listed in the above table is the actual position of the shooting equipment. Since there is a certain distance

between the filming equipment and the bridge, and there is an angular deviation between the direction of the bridge and the filming direction, it is necessary to convert the camera coordinates to the latitude and longitude coordinates corresponding to the center point of the bridge section by the Python algorithm written according to the conversion formula provided in section 3.2.1. The algorithm will automatically calculate the coordinates of the center position of the bridge body corresponding to each image, as shown in Table 4.

Number	Longitude	Latitude
1	116.38998024	39.93508101
2	116.38998055	39.93507832
3	116.38998086	39.93507563
...	...	...

Table 4. Coordinates of the center of the corresponding bridge.

WGS-84 to planar coordinates, As shown in Table 5.

Number	Longitude	Latitude
1	116.38998024	39.93508101
2	116.38998055	39.93507832
3	116.38998086	39.93507563
...	...	...
Number	X	Y
1	447879.4436008291	4420729.996770641
2	447879.4680470604	4420729.698026262
3	447879.4924932939	4420729.399281885
...	...	...

Table 5. WGS-84 to planar coordinates.

Planar coordinates to BIM coordinates : After the above coordinate conversion, the latitude and longitude coordinates of the midpoint of the coordinates of the segmented part of the bridge have been converted to planar coordinates. Because the actual planar coordinates of the bridge and the specific BIM model of the bridge body exist in the translation, rotation, scaling three transformations, so it is necessary to convert the planar coordinates of the midpoint of the coordinates of the segmented part of the bridge body to the coordinates of the model in accordance with 3.2.3.

### 4.3 Identification of Bridge Damages

Each bridge image of the corresponding area of the collected and processed model is used to identify and detect the damage using a deep learning model. Wanning Bridge has a long history and has been carrying the heavy burden of daily transportation. Under such circumstances, flake shedding has become one of the most significant damage problems of Wanning Bridge. In this study, 2568 stone flake shedding images were used to train a deep learning model based on Mask-RCNN. The images are divided into two parts: 80% data for training and 20% for validation. Finally, the trained deep learning model is used to detect and extract the flake shedding from the images of Wanning Bridge collected in this case, as shown in Figure 8.

### 4.4 Damage Information for Integration into BIM Models

Figure 9 shows the locations of the identified flaking damage areas in the image. First, the output mask is converted into a coordinate-recognizable format using Python, and the coordinates are extracted. These identified coordinates are then transformed into a coordinate system with the image center as the



Figure 8. Identified bridge damage.

origin, and all transformed mask coordinates are stored in a database. Next, based on the scale ratio between the image dimensions and the model dimensions, the actual size and position of the damage mask in the model coordinate system are calculated. Each segmented mask coordinate of the flaking damage instances is stored separately. Finally, in Revit's family mode, Dynamo is used to extract the spatial coordinate data of the damage from the database, and a corresponding damage family instance is generated for each mask coordinate. All damage families are then integrated into the original bridge model.

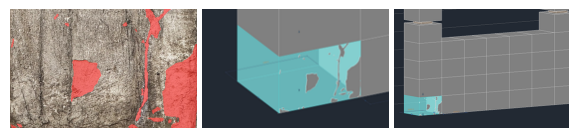


Figure 9. Damage image recognition to model mapping.

## 5. Conclusions

In this study, a set of intelligent detection processes for the damage of stone columns of ancient stone bridges was developed. The system uses handheld devices to take photos of stone bridges, and after processing the photos through image matching technology, deep learning algorithms are utilized to automatically identify the stone damage of stone columns in the photos. The study also designed a set of coordinate conversion schemes, which transform the damage location information recognized in the photos into the actual spatial coordinates in the 3D model and deposit them in the database. Finally, with the help of Dynamo software and Python programming, the damage data was generated into a 3D visualization module, which accurately locates the corresponding position in the bridge model. This system can help the staff visualize the damage of the bridge and provide efficient technical support for the development of protection programs.

## References

- Cheng, M.-Y., Sholeh, M. N., Kwek, A., 2024. Computer vision-based post-earthquake inspections for building safety assessment. *Journal of Building Engineering*, 94, 109909. 10.1016/j.job.2024.109909.
- Delgado, J. M. D., Oyedele, L., Demian, P., Beach, T., 2020. A research agenda for augmented and virtual reality in architecture, engineering and construction. *Advanced Engineering Informatics*, 45, 101122. 10.1016/j.aei.2020.101122.
- Franz, B., Leicht, R., Molenaar, K., Messner, J., 2017. Impact of team integration and group cohesion on project delivery performance. *Journal of construction engineering and management*, 143(1), 04016088. 10.1061/(ASCE)CO.1943-7862.0001219.

- Garrido, I., Lagüela, S., Sfarra, S., Madruga, F., Arias, P., 2019. Automatic detection of moistures in different construction materials from thermographic images. *Journal of Thermal Analysis and Calorimetry*, 138, 1649–1668. 10.1007/s10973-019-08264-y.
- Hawari, A., Alamin, M., Alkadour, F., Elmasry, M., Zayed, T., 2018. Automated defect detection tool for closed circuit television (cctv) inspected sewer pipelines. *Automation in Construction*, 89, 99–109. 10.1016/j.autcon.2018.01.004.
- Huang, H.-w., Li, Q.-t., Zhang, D.-m., 2018. Deep learning based image recognition for crack and leakage defects of metro shield tunnel. *Tunnelling and underground space technology*, 77, 166–176. 10.1016/j.tust.2018.04.002.
- Jeong, G. Y., Nguyen, T. N., Tran, D. K., Hoang, T. B. H., 2020. Applying unmanned aerial vehicle photogrammetry for measuring dimension of structural elements in traditional timber building. *Measurement*, 153, 107386. 10.1016/j.measurement.2019.107386.
- Kaewunruen, S., Rungskunroch, P., Welsh, J., 2018. A digital-twin evaluation of net zero energy building for existing buildings. *Sustainability*, 11(1), 159. 10.3390/su11010159.
- Khan, M. S., Khan, M., Bughio, M., Talpur, B. D., Kim, I. S., Seo, J., 2022. An integrated hbim framework for the management of heritage buildings. *Buildings*, 12(7), 964. 10.3390/buildings12070964.
- Liang, Q., Zhu, W., Sun, W., Yu, Z., Wang, Y., Zhang, D., 2019. In-line inspection solution for codes on complex backgrounds for the plastic container industry. *Measurement*, 148, 106965. 10.1016/j.measurement.2019.106965.
- Lu, Q., Xie, X., Parlikad, A. K., Schooling, J. M., 2020. Digital twin-enabled anomaly detection for built asset monitoring in operation and maintenance. *Automation in Construction*, 118, 103277. 10.1016/j.autcon.2020.103277.
- Lyu, H.-M., Shen, S.-L., Zhou, A., Yang, J., 2019. Perspectives for flood risk assessment and management for mega-city metro system. *Tunnelling and Underground Space Technology*, 84, 31–44. 10.1016/j.tust.2018.10.019.
- O'Byrne, M., Ghosh, B., Schoefs, F., Pakrashi, V., 2020. Applications of virtual data in subsea inspections. *Journal of Marine Science and Engineering*, 8(5), 328. 10.3390/jmse8050328.
- Pocobelli, D. P., Boehm, J., Bryan, P., Still, J., Grau-Bové, J., 2018. BIM for heritage science: a review. *Heritage Science*, 6(1), 1–15. 10.1186/s40494-018-0191-4.
- Pound, M. P., Atkinson, J. A., Townsend, A. J., Wilson, M. H., Griffiths, M., Jackson, A. S., Bulat, A., Tzimiropoulos, G., Wells, D. M., Murchie, E. H. et al., 2017. Deep machine learning provides state-of-the-art performance in image-based plant phenotyping. *Gigascience*, 6(10), gix083. 10.1093/gigascience/gix083.
- Shahi, K., McCabe, B. Y., Shahi, A., 2019. Framework for automated model-based e-permitting system for municipal jurisdictions. *Journal of Management in Engineering*, 35(6), 04019025. 10.1061/(ASCE)ME.1943-5479.0000712.
- Sharafat, A., Khan, M. S., Latif, K., Seo, J., 2021. BIM-based tunnel information modeling framework for visualization, management, and simulation of drill-and-blast tunneling projects. *Journal of Computing in Civil Engineering*, 35(2), 04020068. 10.1061/(ASCE)CP.1943-5487.0000955.
- Wang, T., CHEN, Y.-W., Ishizaki, Y., Miyamoto, M., Hattori, T., 2018. Development of an Image Processing Method for Automatic Inspection of Wear of Throw-away Tips. *Electronics and Communications in Japan*, 101(4), 76–84. 10.1002/ecj.12054.
- Zhang, J., Cheng, J. C., Chen, W., Chen, K., 2022. Digital twins for construction sites: Concepts, LoD definition, and applications. *Journal of Management in Engineering*, 38(2), 04021094. 10.1061/(ASCE)ME.1943-5479.0000948.
- Zhao, J., Feng, H., Chen, Q., de Soto, B. G., 2022. Developing a conceptual framework for the application of digital twin technologies to revamp building operation and maintenance processes. *Journal of Building Engineering*, 49, 104028. 10.1016/j.jobe.2022.104028.
- Zhou, H., Zhao, Y., Shen, Q., Yang, L., Cai, H., 2020. Risk assessment and management via multi-source information fusion for undersea tunnel construction. *Automation in Construction*, 111, 103050. 10.1016/j.autcon.2019.103050.
- Zou, Y., Kiviniemi, A., Jones, S. W., 2017. A review of risk management through BIM and BIM-related technologies. *Safety science*, 97, 88–98. 10.1016/j.ssci.2015.12.027.